

# CHAOS AND ENERGY REDISTRIBUTION IN THE NONLINEAR INTERACTION OF TWO SPATIO-TEMPORAL WAVE TRIPLETS\*

S.R. Lopes<sup>a</sup> and F.B. Rizzato<sup>b†</sup>

<sup>a</sup>*Departamento de Física - Universidade Federal do Paraná, P.O. Box 19081, 81531-990 Curitiba,  
Paraná, Brazil*

<sup>b</sup>*Instituto de Física - Universidade Federal do Rio Grande do Sul, P.O. Box 15051, 91501-970  
Porto Alegre, Rio Grande do Sul, Brazil*

## Abstract

In this paper we examine the spatio-temporal dynamics of two nonlinearly coupled wave triplets sharing two common modes. Our basic findings are the following. When spatial dependence is absent, the homogeneous manifold so obtained can be chaotic or regular. If chaotic, it drives energy diffusion from long to small wavelengths as soon as inhomogeneous perturbations are added to the system. If regular, one may yet have two distinct cases: (i) energy diffusion is again present if the inhomogeneous modes are linearly unstable and triplets are effectively coupled; (ii) energy diffusion is absent if the inhomogeneous modes are linearly stable or the triplets are uncoupled.

---

\*PACS: 05.45.+b; Keywords: Nonlinear Wave Interaction, Hamiltonian Chaos, Spatio-Temporal Chaos, Nonlinear Dynamics

†Telephone: ++ 55-51-3166470; Fax: ++ 55-51-3191762; E-mail: rizzato@if.ufrgs.br

## I. INTRODUCTION

Wave interaction in continuous media is frequently described in terms of amplitude equations. The procedure used to obtain these amplitude equations is standard. Once one identifies a set of high-frequency modes interacting in a resonant fashion, one applies multiple scale formalisms to derive equations governing the slow space-time evolution of these modes; the amplitudes equations.

One of the most investigated types of resonant interaction that can be effectively described by amplitude equations corresponds to the triplet interaction. In that case, three high-frequency modes undergo a resonant interaction which, in the absence of external drives and dissipation, can be shown to produce integrable space-time dependent amplitude equations [1–3].

Another case of resonant interaction that has been attracting some renewed attention is the one involving two coupled triplets sharing two common modes [4–8]. This type of interaction has been shown to produce amplitude equations allowing for temporal chaos [7,8]. To be more specific, if one removes all spatial dependence from the governing equations, then the solutions developing on this *homogeneous manifold* can be chaotic if a number of conditions are fulfilled. Not much, however, has been said about solutions departing from the homogeneous manifold. One relevant question here would be on the stability of the homogeneous manifold against inhomogeneous perturbations. If, for instance, a certain homogeneous solution - not necessarily a static equilibrium - is perturbed with some small inhomogeneity, would this inhomogeneity grow in time? If the answer is positive we would have an *unstable homogeneous manifold*. Otherwise the manifold would be *stable* or *marginally stable*. One could actually split the stability analysis into the analysis of homogeneous manifolds supporting regular dynamics and homogeneous manifolds supporting chaotic dynamics, and the respective results could be significantly different. In fact, as we have observed and shall discuss in detail later, chaotic manifolds are intrinsically unstable. In other words, while regular manifolds may be unstable against some types of perturbation

and stable against others, chaotic manifolds always tend to be unstable no matter the type or strength of the perturbation. What happens in the latter case is that inhomogeneities always tend to grow as a result of the stochastic drive provided by the chaotic orbits evolving on the homogeneous manifold. Here one cannot use linear techniques to investigate stability since the problem is intrinsically nonlinear; one should make use of stochastic models [9] instead. On the other hand, if homogeneous chaos is absent the stochastic drive is absent as well. Then stability can be estimated by linear analysis which in fact shows that only modes falling within the linear instability band are the ones to grow.

Based on these comments one can already see that at least in the case of chaotic homogeneous manifolds, the instability is unlikely to be saturated by any nonlinear effect involving a small number of modes, like soliton formation for instance. As energy is continuously fed into the inhomogeneities, modes with smaller and smaller length scales are eventually excited. Interestingly, we shall also see that in the case of regular homogeneous manifolds coupled to linearly unstable modes, the behavior is similar; the initial instability is not saturated by nonlinear effects involving a finite number of modes and once more energy spreads toward smaller and smaller length scales. Energy flow is arrested only when the triplets are uncoupled, or else when the homogeneous manifold is regular and no inhomogeneous mode falls within the linear instability band.

In view of the previous facts, the issues to be discussed here are related to topics on turbulent motion or on the Fermi-Pasta-Ulam problem [10–12]. Indeed, our homogeneous manifold could be seen as representing fluctuations with very long wavelengths. Therefore the stability problem that we wish to pose here could be more precisely stated as follows: when is our system unstable and under which conditions can energy flow from long to short wavelengths? Contrarily to integrable cases where no flow is observed, we shall see here that *energy transfer* or *energy redistribution* does occur under the conditions mentioned above: (i) when the homogeneous manifold is chaotic; or else (ii) even with a regular homogeneous manifold, when the two triplets are effectively coupled and the inhomogeneous perturbations fall within the instability band.

The paper is organized as follows: in §II we introduce the basic formalism, governing equations, and numerical methodology; in §III we analyze the dynamics on the homogeneous manifold with help of Poincaré maps, in §IV we perform the relevant analyses and simulations for the full spatio-temporal problem, and in §V we conclude the work.

## II. THE MODEL

We are interested in describing the mutual interaction of two wave triplets sharing two common modes and constituted, therefore, by four wave modes in all. We assume that the following resonant conditions are fulfilled:

$$\begin{aligned}
 \omega_{\kappa_1} &\approx \omega_{\kappa_3} + \omega_{\kappa_2}, \\
 \kappa_1 &= \kappa_2 + \kappa_3, \\
 \omega_{\kappa_1} &\approx \omega_{\kappa_4} - \omega_{\kappa_2}, \\
 \kappa_1 &= \kappa_4 - \kappa_2,
 \end{aligned} \tag{1}$$

where  $\omega_{\kappa_j}$  and  $\kappa_j$ ,  $\{j = 1, 2, 3, 4\}$ , are respectively the fast frequencies and fast wavevectors of the interacting waves.

Note that we allow for small frequency mismatches, an usual effect in wave-wave interaction. Frequency mismatch occurs because even for perfectly matched wavevectors, the respective frequencies obtained from the linear dispersion relations may not be quite likewise matched. In laser accelerators and in general laser-plasma interactions, frequency mismatch can even enhance the linear growth rate in several situations [7,13]. Therefore, mismatched modes can be stronger and of greater importance in the dynamics. Moreover, as we shall see here, the integrability properties of the nonlinear regime of the interaction depend critically on the existence of mismatch. Wavevector mismatches could be also incorporated into the theory. However, as frequency and wavevector mismatches are formally equivalent we focus attention on the former.

This type of kinematics where the interacting triplets share two common modes, 1 and 2, has been shown to be of relevance in nonlinear interactions involving electromagnetic, Langmuir and ion-acoustic waves propagating in unmagnetized plasmas [4,7], in magneto-hydrodynamics interactions involving Alfvén and ion-acoustic waves [5], and in plasma-beam interactions in the presence of negative energy waves [6]. Following the model revisited in a series of recent papers [7,8], the dimensionless amplitude equations governing one dimensional, spatio-temporal, slow modulational dynamics can be cast into the form:

$$\frac{\partial A_1(x, t)}{\partial t} + v_{g1} \frac{\partial A_1(x, t)}{\partial x} = A_2(x, t)A_3(x, t) - r A_2^*(x, t)A_4(x, t), \quad (2)$$

$$\frac{\partial A_2(x, t)}{\partial t} + v_{g2} \frac{\partial A_2(x, t)}{\partial x} = -A_1(x, t)A_3^*(x, t) - r A_1^*(x, t)A_4(x, t), \quad (3)$$

$$\frac{\partial A_3(x, t)}{\partial t} + v_{g3} \frac{\partial A_3(x, t)}{\partial x} = i\delta_3 A_3(x, t) - A_1(x, t)A_2^*(x, t), \quad (4)$$

$$\frac{\partial A_4(x, t)}{\partial t} + v_{g4} \frac{\partial A_4(x, t)}{\partial x} = i\delta_4 A_4(x, t) + r A_1(x, t)A_2(x, t). \quad (5)$$

$A_j$ ,  $\{j = 1, 2, 3, 4\}$ , are the complex amplitudes of the four fields,  $\delta_{3,4} = \omega_1 \mp \omega_2 - \omega_{3,4}$  are independent frequency mismatches corresponding to fields  $A_3$  and  $A_4$  (i.e., one can always take  $\delta_1 = \delta_2 = 0$ , as we actually did),  $r$  is a variable strength factor measuring the intensity of the triplet-triplet coupling [7,8], and  $v_{g_j}$  are the respective group velocities along the spatial modulation that we take as one dimensional (the  $x$  axis) in this work. Time and space derivatives are first order as a result of our multiple time and space scales.

The set of governing equations (2)-(5) can be derived from a continuous Hamiltonian. Indeed, it is possible to see that the following relations hold

$$\frac{\partial A_j(x, t)}{\partial t} = \frac{\delta H}{\delta A_j^*}, \quad \frac{\partial A_j(x, t)^*}{\partial t} = -\frac{\delta H}{\delta A_j}, \quad (6)$$

where we introduce the functional derivative

$$\frac{\delta}{\delta A_j} \equiv \frac{\partial}{\partial A_j} - \frac{\partial}{\partial x} \frac{\partial}{\partial (\frac{\partial A_j}{\partial x})} \quad (7)$$

(the same definition holds if  $A$  is replaced with  $A^*$ ), and where the Hamiltonian is to be written in the form

$$H = \int dx [-A_1 A_2^* A_3^* + A_1^* A_2 A_3 - r(A_1^* A_2^* A_4 - A_1 A_2 A_4^*) + i\delta_3 |A_3|^2 + i\delta_4 |A_4|^2 - \sum_{j=1}^4 v_{g_j} A_j^* \frac{\partial A_j}{\partial x}]. \quad (8)$$

The Hamiltonian does not depend explicitly on time; therefore it is a time conserved quantity.

In addition to the Hamiltonian, the following quantities are also conserved:

$$C_1 = \int dx [ |A_2|^2 - |A_3|^2 + |A_4|^2 ], \quad (9)$$

$$C_2 = \int dx [ |A_1|^2 + |A_3|^2 + |A_4|^2 ], \quad (10)$$

and they suggest that we can look at the whole process as a decay interaction with  $A_1$  as the decaying pump; from this perspective,  $A_2$  is an idler wave whereas  $A_3$  is a Stokes mode and  $A_4$  an anti-Stokes mode. In the case of nonlinear interactions in unmagnetized plasmas for instance, wave  $A_1$  is a transverse electromagnetic wave, wave  $A_2$  is ion-acoustic, and waves  $A_3$  and  $A_4$  are Stokes and anti-Stokes Langmuir modes [4,7].

All those quantities will be useful in checking out the accuracy of our integration methods which we outline now. The basic integration method is pseudo-spectral and the four fields  $A_j$ ,  $\{j = 1, 2, 3, 4\}$ , are Fourier analyzed according to

$$A_j = \sum_{n=-N/2+1}^{N/2} a_{j_n}(t) e^{inkx}. \quad (11)$$

For further purposes note that while  $j$  denotes the *wave type*,  $n$  denotes the *mode number* or *harmonic number*. The harmonic or modal amplitudes  $a_{j_n}$  are integrated in time with a predictor-corrector algorithm. We use  $N = 64, 128, 256$  modes removing half of them to cure aliasing. We denote the basic slow wavevector by  $k$  and point out that due to the structure of the equations, variations in  $k$  can be absorbed in variations of the group velocities or vice-versa. Fluctuations of the conserved quantities, including energy, are not larger than one part in  $10^7$ , and variations of the tolerance factors of the integrator do not alter the final outcome of the runs.

### III. DYNAMICS ON THE HOMOGENEOUS MANIFOLD

As a first step let us analyze the behavior of the dynamics on the homogeneous manifold. The motivation and relevance of a consistent analysis of the homogeneous dynamics has been commented in the Introduction and has roots in the stochastic pump model that we discuss next. According to the stochastic pump model [9], as soon as strongly chaotic degrees-of-freedom of a dynamical system are coupled to additional degrees-of-freedom, the chaotic subsystem acts like a stochastic pump delivering a net amount of energy to its environment. This net energy transfer is diffusive and takes place at all because of the very random nature of the coupling. In a certain sense, the dynamics is equivalent to the coupling of two thermodynamical systems, one cold and the other hot. As a result of the random coupling, a net energy transfer finally equalizes the temperatures of both systems. In our case, the hot system would be the chaotic homogeneous manifold and the cold one the subset of the inhomogeneous modes. Furthermore, and precisely due to diffusion, energy would be redistributed over the accessible phase-space of the inhomogeneous modes exciting progressively harmonics with finer and finer length scales.

Homogeneous orbits have been recently investigated in a paper by Pakter, Lopes, & Viana [8]. Let us review the basic results and take the opportunity to introduce a convenient notation to be used here. To investigate the types of orbits on the homogeneous manifold, let us thus assume that we are working with fields of the form

$$A_j(x, t) \equiv a_{j_o}(t), \quad (12)$$

which do not depend on the spatial coordinate. Then, introducing real amplitudes and phases through

$$a_{j_o} = \sqrt{\rho_j} e^{i\phi_j}, \quad \{j = 1, 2, 3, 4\}, \quad (13)$$

one obtains canonical conjugate equations for these quantities, with a reduced governing Hamiltonian  $h$  given in the form

$$h = 2\sqrt{\rho_1\rho_2\rho_3} \sin(\phi_1 - \phi_2 - \phi_3) - 2r\sqrt{\rho_1\rho_2\rho_4} \sin(\phi_1 + \phi_2 - \phi_4) - \delta_3\rho_3 - \delta_4\rho_4. \quad (14)$$

This type of Hamiltonian structure has been largely studied in the context of nonlinear waves [14]. What we learn is that due to the particular phase combinations of the sine functions, a number of relatively simple canonical transformations can be applied to simplify the problem. The first transformation introduces a new phase angle  $\phi'_1$  in the form  $\phi'_1 = \phi_1 - \phi_2 - \phi_3$  and preserves the other phases,  $\phi'_j = \phi_j$ ,  $\{2, 3, 4\}$ . Rewriting conveniently the argument of the second sine function of expression (14), the form of the second canonical transformation becomes clear; it shall be constructed such as to introduce a new phase angle  $\phi''_4 = \phi'_4 - 2\phi'_2 - \phi'_3$ , preserving all the others  $\phi''_j = \phi'_j$ ,  $\{j = 1, 2, 3\}$ . As a result of the pair of transformations described above, one finally arrives at

$$\rho_2 = \rho''_2 - \rho''_1 - 2\rho''_4, \quad (15)$$

$$\rho_3 = \rho''_3 - \rho''_1 - \rho''_4, \quad (16)$$

and

$$h = 2\sqrt{\rho_1(\rho_2 - \rho_1 - 2\rho_4)(\rho_3 - \rho_1 - \rho_4)} \sin(\phi_1) - 2r\sqrt{\rho_1\rho_4(\rho_2 - \rho_1 - 2\rho_4)} \sin(\phi_1 - \phi_4) - \delta_3(\rho_3 - \rho_1 - \rho_4) - \delta_4\rho_4, \quad (17)$$

where the double primes have been dropped in the Hamiltonian (17). Since the Hamiltonian no longer depends on coordinates  $\phi_2$  and  $\phi_3$ , the associated momenta  $\rho_2$  and  $\rho_3$  are constants of motion with their relation to the original variables given by relations (15) and (16). Furthermore, the Hamiltonian  $h$ , Eq. (17), is a conserved quantity itself since it does not depend explicitly on time. We now focus attention on conditions allowing for decay processes where  $A_1$  is to be considered a pump wave. In the decay case one requires  $A_1 \neq 0$  and  $A_2 = A_3 = A_4 = 0$ , which implies, in view of conditions (12)-(17), that our energy surface of interest here is actually indexed by  $h = 0$ .

The flow governed by  $h$  is two-degrees-of-freedom and thus likely to be nonintegrable [9]. The relevant governing equations obtained from Hamiltonian (17) are:

$$\begin{aligned} \frac{d\rho_1}{dt} &= -2\sqrt{\rho_1(\rho_2 - \rho_1 - 2\rho_4)(\rho_3 - \rho_1 - \rho_4)} \cos \phi_1 \\ &\quad + 2r\sqrt{\rho_1\rho_4(\rho_2 - \rho_1 - 2\rho_4)} \cos(\phi_1 - \phi_4), \end{aligned} \quad (18)$$

$$\frac{d\rho_4}{dt} = -2r\sqrt{\rho_1\rho_4(\rho_2 - \rho_1 - 2\rho_4)} \cos(\phi_1 - \phi_4), \quad (19)$$

$$\begin{aligned} \frac{d\phi_1}{dt} &= \frac{1}{\sqrt{\rho_1(\rho_2 - \rho_1 - 2\rho_4)(\rho_3 - \rho_1 - \rho_4)}} \sin \phi_1 \times \\ &\quad \left[ \rho_2\rho_3 - 2\rho_1\rho_2 - \rho_2\rho_4 - 2\rho_1\rho_3 + 3\rho_1^2 + 6\rho_1\rho_4 - 2\rho_4\rho_3 + 2\rho_4^2 \right] - \\ &\quad \frac{r \sin(\phi_1 - \phi_4)}{\sqrt{\rho_1\rho_4(\rho_2 - \rho_1 - 2\rho_4)}} \left[ \rho_4\rho_2 - 2\rho_1\rho_4 - 2\rho_4^2 \right] + \delta_3, \end{aligned} \quad (20)$$

and

$$\begin{aligned} \frac{d\phi_4}{dt} &= \frac{1}{\sqrt{\rho_1(\rho_2 - \rho_1 - 2\rho_4)(\rho_3 - \rho_1 - \rho_4)}} \sin \phi_1 \times \\ &\quad \left[ -2\rho_1\rho_3 + 3\rho_1^2 + 4\rho_1\rho_4 - \rho_1\rho_2 \right] - \\ &\quad \frac{r \sin(\phi_1 - \phi_4)}{\sqrt{\rho_1\rho_4(\rho_2 - \rho_1 - 2\rho_4)}} \left[ \rho_1\rho_2 - \rho_1^2 - 4\rho_1\rho_4 \right] + \delta_3 - \delta_4. \end{aligned} \quad (21)$$

However there is at least one pair of limiting cases where the dynamics becomes completely integrable. One of them occurs when  $\delta_3 = \delta_4 = 0$ . In this situation Romeiras [15] has identified a new constant of motion that reduces the system to one-degree-of-freedom. The other integrable limit occurs when  $r \rightarrow 0$ ; in this situation mode  $A_4$  decouples from the multiplet and one recovers the pure three wave decay which, again, is one-degree-of-freedom and hence completely integrable.

To understand and visualize the properties and characteristics of the purely homogeneous interaction, let us fix  $r = 1.0$  - a typical condition of interactions processing in unmagnetized plasmas or magnetohydrodynamics environments, for instance - and  $\delta_4 = 0$ . Let us then

proceed to investigate the system behavior as  $\delta_3$  is allowed to vary. We make use of Poincaré plots, where we record the values of  $\rho_1$  and  $\phi_1$ , as determined by the governing reduced Hamiltonian (17), each time  $d\rho_4/dt = 0$  with  $d^2\rho_4/dt^2 > 0$ . We consider weak nonlinearities and launch a number of initial conditions, in fact 10, under the constraint  $h = 0$ . In all the conditions we take  $\phi_1 = \pi/2$ ,  $\phi_4 = 0$ ;  $\rho_1$  is uniformly distributed within a weakly nonlinear range  $0 < \rho_1 < \rho_{max} < 1$  and  $\rho_4$  is calculated from  $h = 0$ . Finally, to be consistent with typical decay conditions, we take  $\rho_2 = \rho_3 = \rho_{max}$  such that whenever  $\rho_1 = \rho_{max}$  and  $\rho_4 = 0$ ,  $A_2 = A_3 = 0$ .

As mentioned, in this paper we investigate weakly nonlinear regimes; all the simulations are performed with  $\rho_{max} = 0.1$ . Now the first plot shown in Fig. (1a) is produced for parameters lying in an essentially regular regime where  $r = 1$ , and  $\delta_3 = 0.0001$ . As predicted by Romeiras [15], for such a small  $\delta_3$  the phase-space is essentially regular displaying a series of closed curves that in fact reveal the existence of numerous invariant KAM (Kolmogorov-Arnold-Moser) tori [9]. Then, as we increase the value of the mismatch up to  $\delta_3 = 0.1$ , Fig. (1b) indicates that the KAM tori become substantially eroded; chaos is strong in this case. As we couple the homogeneous manifold to inhomogeneous perturbations, diffusion towards small wavelengths is expected to occur in the latter situation.

We have therefore obtained some initial information on the behavior of the homogeneous manifold. But the real question yet to be answered is how that kind of behavior on this manifold affects the inhomogeneous dynamics. We shall address this issue next.

#### IV. FULL SPATIO-TEMPORAL DYNAMICS

The typical initial conditions to be used in this paper place the homogeneous orbits on the outermost curve of Fig. (1a), close to a separatrix orbit containing two unstable fixed points located at the maximum  $\rho_1$  - in this case  $\rho_1 = 0.1$  - and  $\phi_1 = 0, \pi$ . These fixed points represent the exact homogeneous equilibria of our system. In regular cases the orbit remains close to the separatrix and since the separatrix orbit spends an infinitely large amount of

time close to the fixed points, we estimate linear stability simply by replacing the actual orbit with the fixed points. The estimates shall be shown to be accurate enough when compared with the simulations.

Let us thus suppress for a little while the dynamics on the homogeneous manifold and assume that we have an equilibrium situation characterized by  $A_1^{(0)} = a_{10}^{(0)} \equiv \mathcal{A} \neq 0$  ( $\mathcal{A}$  is a complex constant), and  $a_{j_n}^{(0)} = 0, \{j = 2, 3, 4\}$ , for any other  $n$ . As mentioned before, this is the convenient condition if one wishes to study the stability of a strong pump - mode  $A_1$  - feeding vanishingly small modes - modes  $A_j, \{j = 2, 3, 4\}$ . The stability of the pump can then be readily investigated if one adds small perturbations  $A_j^{(1)} = a_{j1}^{(1)} e^{ikx}, a_{j1}^{(1)} \sim e^{-i\Omega t}$  to the system. Indeed, if  $|a_{j1}^{(1)}| \ll |A_1^{(0)}|$ , a dispersion relation  $\Omega = \Omega(k)$  can be obtained from

$$P_3 P_2 - P_R = 0, \tag{22}$$

where

$$P_3 = i(-\Omega + v_{g3}k - \delta_3),$$

$$P_2 = i(-\Omega + v_{g2}k),$$

$$P_R = |\mathcal{A}|^2 \left(1 - r^2 \frac{P_3}{P_4}\right),$$

$$P_4 = i(-\Omega + v_{g4}k - \delta_4).$$

The dispersion relation (22) can be analyzed numerically but here we abbreviatedly discuss some of its relevant results. For a given  $\mathcal{A}$ , there exists an instability (complex  $\Omega$ 's) band extending from  $k = 0$  up to a certain  $k_{max}$ . The larger the value of  $\mathcal{A}$ , the larger  $k_{max}$ , but otherwise the instability band is not strongly dependent on  $\delta_3, \delta_4$ , and  $r$ . The instability for  $k = 0$ , in particular, is the one giving rise to the homogeneous dynamics that was the subject of study in section II and in previous works [7,8]. As a relevant information obtained there, we recall that the ensuing homogeneous dynamics can be chaotic or regular depending on the initial conditions and control parameters.

We can now collect the results obtained so far to assert that in general we have four global types of situations to be investigated. These four situations result from the four

distinct associations involving a regular *or* chaotic homogeneous manifold, with inhomogeneous perturbations launched inside *or* outside the linear instability band. Our interest is to discover in which of the four situations can one detect energy diffusion from long to small wavelengths. Although all four cases are of interest, in this paper we shall focus on the two independent situations that provide a clear view on the individual role of the basic nonlinear effects driving diffusion: chaotic homogeneous manifolds associated with linearly stable inhomogeneous perturbations, and regular homogeneous manifolds associated with linearly unstable inhomogeneous perturbations. The behavior of the two remaining cases may be then obtained by an extension of the behavior of these basic ones. Our classification outlined above may sound artificial since the homogeneous and inhomogeneous dynamics are in fact coupled and mutually interactive; in other words they should not be considered apart from each other in principle. However, the classification adopted explains well enough what we are about to see: in the case of chaotic homogeneous manifolds coupled to stable modes, the diffusion is so slow that at any instant one can consider the chaotic dynamics as adiabatically delivering energy to the inhomogeneous modes; in the case of regular homogeneous manifolds coupled to unstable modes, similarly, a possible regular dynamics on the homogeneous manifold does not alter significantly the results of linear stability calculations.

To monitor instabilities and energy transfer, we make use of a spectral average [16,17] that enables to estimate the number of active modes in the system. We denote this quantity by  $\sqrt{\langle N^2 \rangle}$  and define it as

$$\sqrt{\langle N^2 \rangle} = \sqrt{\frac{\sum_{n=-N/2+1}^{N/2} \sum_{j=1}^4 n^2 |a_{jn}|^2}{\sum_{n=-N/2+1}^{N/2} \sum_{j=1}^4 |a_{jn}|^2}}. \quad (23)$$

From its definition one sees that  $\sqrt{\langle N^2 \rangle}$  is the square root of the averaged  $n^2$ . The average is taken over mode number ( $n$ ) and mode type ( $j$ ), and weighted by the square of the mode amplitude for a fixed initial condition. One could also average over several similar initial conditions but our results on energy transfer remain the same as long as the initial conditions are all simultaneously stable or all simultaneously unstable.  $\sqrt{\langle N^2 \rangle}$  is expected to grow in time in diffusive cases where more and more modes become involved in

the dynamics. In the absence of energy transfer,  $\sqrt{\langle N^2 \rangle}$  remains limited by the number of linearly unstable modes; in the case of stable modes only,  $\sqrt{\langle N^2 \rangle} \rightarrow 0$ .

In our simulations we take  $\delta_4 = 0$ . Our results on energy transfer are qualitatively independent of a precise choice of group velocities. Therefore we consider  $v_{g_j} = 0$ ,  $\{j = 1, 3, 4\}$  for simplicity, since variations of  $v_{g_2}$  alone provides an easy way to control the width of the band of linear instability. We point out that a precise choice of velocities would be essential either in the case of a pure triplet interaction, or else if one were performing a detailed study of how the dynamics of the four-wave system evolves in time during intermediary stages, as the asymptotic state is approached. Indeed, depending on the ordering of group velocities solitons can actually saturate the pure triplet interaction or perhaps can serve as metastable intermediary states existing for a finite amount of time when a fourth wave destroying integrability is added. However, once the four-wave system has a chaotic homogeneous manifold or becomes linearly unstable as discussed earlier, energy transfer progresses regardless the presence or absence of solitons in these intermediary states. Note that when the coupling parameter  $r$  is sufficiently large, the dynamics of the four-wave system does not resemble that of the triplet interaction. This is why we adopt the simple ordering discussed above; other orderings not presented in the present work have been tested as well.

In any case, such a choice is of physical significance for the interaction of electromagnetic, ion-acoustic and Langmuir waves in plasmas with small enough Debye length. In that case one shows that the only relevant group velocity is the one corresponding to the ion-acoustic mode, the  $A_2$  wave [7]. The choice of the numerical value for  $v_{g_2}$  and  $k$  is arbitrary to a large extent. This is due to the structure of the governing equations (2)-(5), which are invariant under the rescalings

$$v_{g_j} \rightarrow \alpha v_{g_j}, \quad x \rightarrow \alpha x \tag{24}$$

and

$$A_j \rightarrow \beta A_j, \quad t \rightarrow \frac{t}{\beta}, \quad x \rightarrow \frac{x}{\beta}, \quad \delta_j \rightarrow \beta \delta_j, \quad \{j = 1, 2, 3, 4\}, \tag{25}$$

$\alpha$  and  $\beta$  being independent scale factors. This fact effectively creates some additional freedom in choosing the simulation parameters. Here we shall consider  $k = 1.0$  in all cases.

### A. The $\delta_3 \neq 0$ case.

Let us consider as a first instance the case of a chaotic homogeneous manifold combined with linearly stable perturbations. To simulate this situation, we use the same parameters and techniques employed to construct Fig. (1b). In the homogeneous manifold the initial condition corresponds to the outermost orbit present in the figure. Since we had launched 10 equally spaced orbits, a rapid calculation therefore shows that the value of  $\rho_1(t = 0)$  to be used in the simulation reads  $\rho_1(t = 0) = 0.09$ . Fig. (1b) also shows that we take  $\phi_1(t = 0) = \pi/2$  for the initial phase. In addition we recall that  $\phi_4 = 0$  and  $h = 0$ . Note that the relations between  $\rho$ 's,  $\phi$ 's and  $a_{j_0}$  are the same as previously defined in Eq. (13). For the inhomogeneous perturbation, besides  $k = 1.0$ , we take  $v_{g_2} = 1.0$  as the relevant group velocity. The perturbing field itself is written in the form  $Re[a_{11}] = |a_{10}| \times 10^{-3}$ ,  $Im[a_{11}] = |a_{10}| \times 10^{-3}$  where  $Re[\bullet]$  and  $Im[\bullet]$  respectively denote real and imaginary parts of the various fields. For this particular choice of parameters and initial conditions, the inhomogeneous perturbations alone would be linearly stable, since here we have  $k_{max} \approx 0.4 < k = 1.0$ . On the other hand the low-dimensional phase-space is chaotic, and because of this fact, some kind of energy transfer should be expected after all. The initial results of our simulations can be found in Fig. (2). It is clearly seen that in spite of the linear stability of the system, transfer does indeed occur as  $\sqrt{\langle N^2 \rangle}$  continuously grow until it reaches saturation due to the finite number of modes used in the numerical code. What happens here can be understood in terms of the stochastic pump model mentioned before, and discussed, for instance, in the book of Lichtenberg & Lieberman [9]. The strong chaotic dynamics developing at  $k = 0$  acts like a random force, diffusively driving all the remaining modes of the system. It does not matter if these remaining modes are linearly stable. What really matters is that as a result of the stochastic pump the inhomogeneous modes start to

be driven similarly to what would happen if they were in contact with a thermal reservoir. Simulations with other values of  $\delta_3$  are also shown in Fig. (2). It is seen that as one lowers  $\delta_3$ , redistribution weakens. In the limit of very small values of the mismatch, one recovers the situation depicted in Fig. (1a) where the homogeneous manifold is regular. Then diffusion apparently ceases or becomes very slow, what leads us to draw a most expected conclusion on the features of the system: when the homogeneous manifold is regular and no harmonic mode falls within the linear instability band, diffusion is negligible.

Figure (3a) shows that the larger the number of modes used in the simulations, the larger the saturated value of  $\sqrt{\langle N^2 \rangle}$ . In other words there is no nonlinear saturating effect that involves only a small and fixed number of modes. In addition to that, the various numbers of modes used in the figure,  $N = 64, 128, \text{ and } 256$ , indicate that diffusion is not an effect connected with the finite discretization of the numerical method. Diffusion is present no matter the value of  $N$ . One can see this because for earlier times of the nonlinear interaction where a few modes are actually excited, the behavior of all curves are virtually the same. A close inspection of the final spectral-energy distribution reveals that our asymptotic states are not quite fully equipartitioned in energy. Although the spectral distribution for large mode numbers is relatively flat, the energetic content in the spectral region of small mode numbers is slightly larger. This can be seen with help of Fig. (3b) where we plot the energy of the free-modes,  $E_n = \ll (\delta_j + nk) |a_{j_n}|^2 \gg$ , doubly averaged over time and over the wave index  $\{j = 1, 2, 3, 4\}$ . This discrepancy between full equipartition and simulations could have two contrasting sources that should be investigated: either the wave amplitudes we work with are already so high that the interaction term is no longer a small perturbation, or for the parameters used here integrable features are still appreciable. It is perhaps convenient to mention that the convergence of the spectral distribution has been verified by extending and reducing the averaging time interval in various ways; for sufficiently long intervals the results are the same.

To complement the information obtained with help of Figs. (2) and (3), in Fig. (4) we display the space-time history of  $|A_1(x, t)|$  corresponding to the  $\delta_3 = 0.1$  curve of Fig.

(2). It may be seen that for earlier times of the nonlinear interaction, one has a purely time dependent solution that is completely homogeneous in space. However, as time is let to evolve, strong spatial oscillations adds to the previous erratic but pure time dependence. The upper time limit of the simulation is  $t = 20000$  which is smaller than the asymptotic time where the system reaches saturation. Nevertheless, it is clear from the figure that inhomogeneities are already strongly excited by then.

### B. The $\delta_3 = 0$ case.

Now let us consider the other individually relevant situation in which we combine a regular manifold with a linearly unstable perturbation. The relevant graphical information can be found in Fig. (5). In this case we work with  $\delta_3 = 0$  so as to guarantee that the homogeneous manifold is in fact regular. The choice of initial conditions follows the pattern used to construct the previous figures. We launch 10 initial conditions on the homogeneous manifold equally spaced between  $\rho_1 = 0$  and  $\rho_{max} = 0.1$ , and select the initial condition for the full simulations as the one corresponding to the outermost orbit with  $\phi_1 = \pi/2$ . We choose  $v_{g_2} = 0.06$  such as to have at least some linearly unstable modes. In fact, within the range of variation of  $r$  in the figure, use of Eq. (22) shows that the number of unstable modes is approximately 5 for all cases.

One could think that as chaotic activity is absent from the homogeneous manifold, no diffusion would be observed now. This proves to be untrue. Indeed, Fig. (5) shows that when  $r \neq 0$ , energy diffusion is *again* present, even though homogeneous chaos is not (remember that  $\delta_3 = 0$ ). We had seen before that for coupled triplets - that is if  $r \neq 0$  - purely temporal chaos alone is capable to drive energy redistribution, even though inhomogeneous perturbations are linearly stable. Now what we are observing is a complementary effect. Namely, unstable inhomogeneous modes alone are capable to drive redistribution if  $r \neq 0$  even though the homogeneous manifold is integrable ( $\delta_3 = 0$ ). In this case the active modes cannot be excited with the stochastic pump simply because there is no stochastic pump

available. Instead they are excited by the linear instability of the system, and as soon as they are excited diffusion starts to operate again. This feature leads us to reconsider the first case analyzed here. In fact, in this first case where we have a chaotic homogeneous manifold combined with stable spatial modes diffusion can be understood in terms of the stochastic pump model only for earlier times of the nonlinear interaction, when the inhomogeneity is relatively small. Only then are the effects of the spatial inhomogeneities small, with diffusion totally dictated by the homogeneous chaos. As soon as the inhomogeneous fluctuations grow larger, both nonintegrable effects become of the same order of magnitude. At this stage the overall dynamics should become similar to that case where one combines a chaotic manifold with unstable inhomogeneous modes, a case not individually explored in this work.

## V. FINAL REMARKS

A general comment is that in the wide sense investigated here, the global stability of the homogeneous manifold cannot be simply understood in terms of a linear stability analysis. In fact, we have shown explicitly that the linear analysis fails when the homogeneous manifold is chaotic. To emphasize our point we have analyzed a particular setting where the inhomogeneous modes that we have launched are linearly stable. Even so, inhomogeneous perturbations tend to grow as time evolves. What happens in this case is that at least for earlier times of the nonlinear interaction, the chaotic homogeneous manifold acts like a stochastic pump delivering energy in a random fashion to these inhomogeneous modes. One calls that situation the stochastic pump because the role of the homogeneous manifold is comparable to the role of a thermal reservoir diffusively delivering energy to its vicinities [9,11].

When homogeneous chaos is absent, two types of behaviors could be identified for  $r \neq 0$ . If no inhomogeneous perturbation falls within the band of linear instability, then the system does not develop any sort of configuration with spatial dependence and simply keeps supporting a homogeneous periodic dynamics. On the other hand, when at least one of the

inhomogeneous modes does fall within the instability band one has again diffusion towards small spatial scales. This shows that the nonintegrable features of our system are not exclusively related to the temporal dynamics developing on the homogeneous manifold. In the homogeneous manifold, chaos vanishes as  $\delta_3 \rightarrow 0$ , but for dynamical states involving unstable modes with  $k \neq 0$ , energy redistribution is present irrespectively of the value of  $\delta_3$ . In other words, even if  $\delta_3 = 0$  in these situations, random activity is still present.

The spatio-temporal dynamics of one isolated wave triplet has been shown to be integrable via inverse-scattering [1,3]. Our results indicate that as one couples a fourth wave such as to form two wave triplets sharing two common modes, integrability breaks down. What seems to be happening here is that as one couples the fourth mode, the regular solutions of the isolated triplet undergo a transition to chaos. Then, the resulting chaotic dynamics enhances radiative effects and causes energy transfer to modes with larger and larger wavevectors; this and the following are issues under current investigation. The regular asymptotic dynamics of the pure triplet is somewhat related to the intermediary dynamical stages of the four-wave system. Consider, for instance, an ordering of group velocities for which solitons saturate the pure triplet interaction, as commented earlier. When the fourth-wave is coupled to the unperturbed triplet, integrability is destroyed and solitons survive only for finite amounts of time, ultimately releasing their energy into small scale fluctuations. In other words, regular structures that are the final asymptotic states of the triplet interaction, are present only during intermediary stages of the full four-wave system. In addition, although the ordering of the group velocity is relevant during intermediary stages of the full interaction, we see that it is not expected to drastically affect the asymptotic dynamics and the overall process of energy transfer: eventually modes with short spatial scales are excited and intermediary regular structures are no longer present in the system.

Another important point to be considered is that the general technique of multiple time scales leading to generic amplitude equations breaks down when modes with large enough wavevectors become involved in the dynamics. Then, dispersive and dissipative effects should be included since these terms are always related to small wavelengths - dispersion because it

appears in the form of derivatives terms like  $\partial^2 A_j / \partial x^2$  such that the smaller the length scale, the larger the derivative, and dissipation because it occurs when the waves strongly interact with small scale structures of the global system, like for example high-velocity particles in plasmas. While we are currently considering these points, we emphasize that our present model works well for earlier times of energy transfer when modes with small wavelengths are still of very small amplitudes. In particular, all the conditions analyzed here that engage transfer, involve only large wavelengths and are therefore fairly accurate.

### ACKNOWLEDGMENTS

We would like to thank nice discussions with R. Pakter, A. Chian, and R. Viana. We also thank suggestions from two anonymous referees. This work was partially supported by Financiadora de Estudos e Projetos (FINEP), Conselho Nacional de Desenvolvimento Científico e Tecnológico (CNPq), and Fundação da Universidade Federal do Paraná (FUNPAR), Brazil. Numerical computing was performed on the CRAY Y-MP2E at the Universidade Federal do Rio Grande do Sul Supercomputing Center.

## REFERENCES

- [1] D.J. Kaup, A.H. Reiman, and A. Bers, Rev. Mod. Phys. **51** (1979) 275.
- [2] J. Weiland and H. Wilhelmsson, “*Coherent Non-Linear Interaction of Waves in Plasmas*”, Pergamon Press (1977).
- [3] C.C. Chow, Physica D **81** (1995) 237.
- [4] R. Sugihara, Phys. Fluids **11** (1968) 178.
- [5] K.S.Karplyuk, V.N. Oraevskii, and V.P. Pavlenko, Plasma Phys. **15** (1973) 113.
- [6] D. Walters and G.J. Lewak, J. Plasma Phys. **18** (1977) 525.
- [7] A.C.-L. Chian, S.R. Lopes, and J.R. Abalde, Physica D, **99** (1996) 269.
- [8] R. Pakter, S.R. Lopes, and R. Viana “*Transition to Chaos in the Conservative Four-Wave Parametric Interactions*” Physica D *accepted* (1997).
- [9] A.J. Lichtenberg and M.A. Lieberman, “*Regular and Stochastic Motion*”, Springer (1983).
- [10] M. Pettini and M. Landolfi, Phys. Rev. A **41** (1990) 768.
- [11] C.G. Goedde, A.J. Lichtenberg, and M.A. Lieberman, Physica D **59** (1992) 200.
- [12] G. Tsaur and J. Wang, Phys. Rev. E **54** (1996) 4657.
- [13] F.B. Rizzato and A.C.-L. Chian, J. Plasma Phys. **48** (1992) 71; R. Pakter, R.S. Schneider, and F.B. Rizzato, Phys. Rev. E **49** (1994) 1594.
- [14] G.I. de Oliveira, L.P.L. de Oliveira, and F.B. Rizzato, Physica D **104** (1997) 119.
- [15] F.J. Romeiras, Phys. Lett. **93A** (1983) 227.
- [16] D.U. Martin and H.C. Yuen, Phys. Fluids **23** (1980) 1269.
- [17] A. Thyagaraja, Phys. Fluids **24** (1981) 1973.

## FIGURES

FIG. 1. Poincaré plots on the homogeneous manifold for  $r = 1.0$ :  $\delta_3 = 0.0001$  in (a) and  $\delta_3 = 0.1$  in (b)

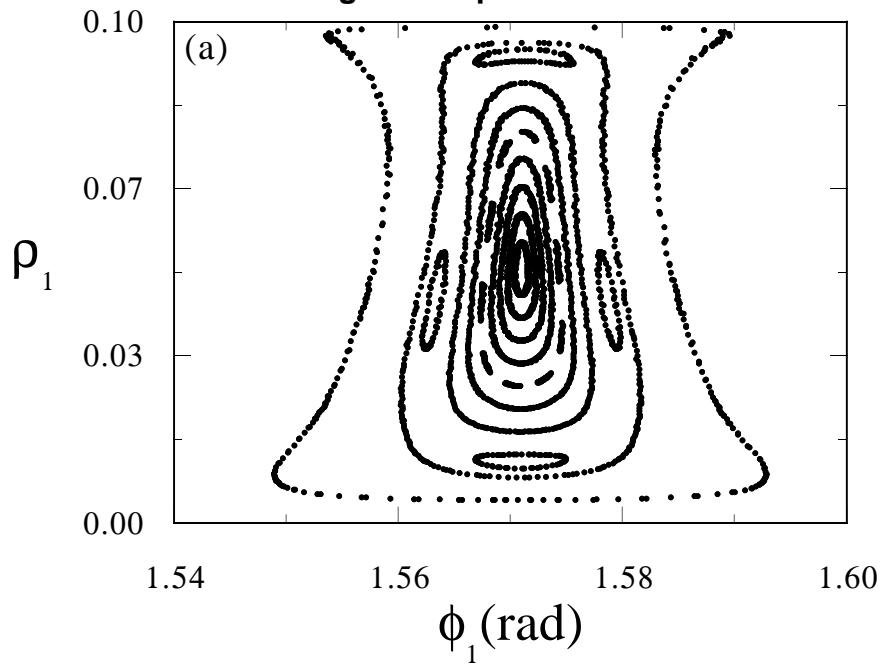
FIG. 2. Time series of  $\sqrt{\langle N^2 \rangle}$  for  $r = 1.0$ ,  $v_{g_2} = 1.0$ ,  $N = 128$ , and various values of  $\delta_3$ . Initial conditions discussed in the text.

FIG. 3. (a) Comparison of time series of  $\sqrt{\langle N^2 \rangle}$  for different number of modes used in the simulations; (b) Spectral-energy distribution of the case  $N = 256$  above, averaged over time and over the mode index  $j$ . In all cases  $\delta_3 = 0.1$ ,  $r = 1.0$ ,  $v_{g_2} = 1.0$ ; initial conditions discussed in the text.

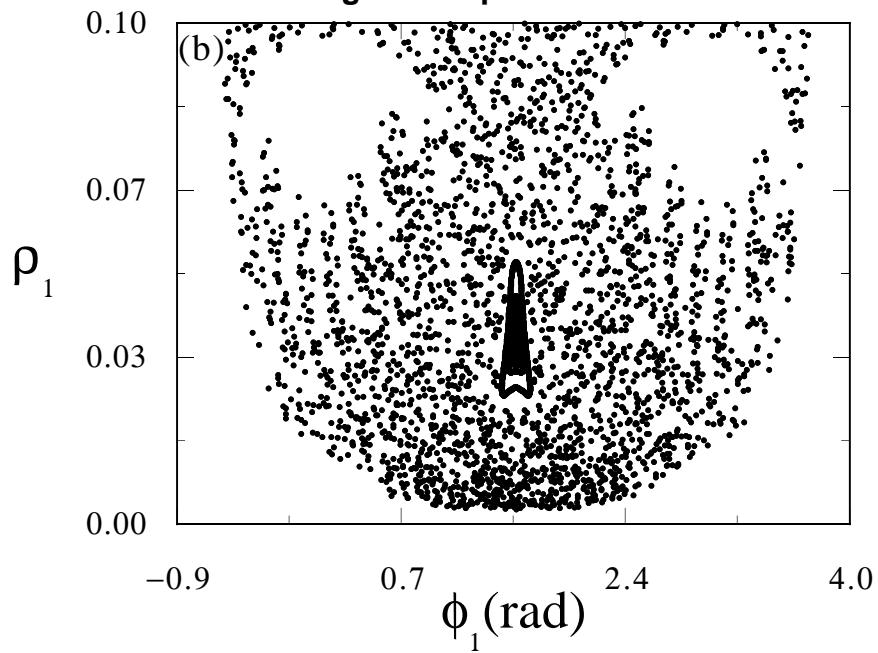
FIG. 4. Space-time history of  $|A_1(x, t)|$  for the  $\delta_3 = 0.1$  case of Fig. (2). By the end of the simulation inhomogeneities are already strongly excited.

FIG. 5. Time series of  $\sqrt{\langle N^2 \rangle}$  when orbits of the regular type evolve on the homogeneous manifold. The number of linearly unstable modes in all cases is approximately 5. In all cases  $\delta_3 = 0$ ,  $v_{g_2} = 0.06$  and  $N = 128$ ; initial conditions discussed in the text.

**Fig.1a: Lopes & Rizzato**



**Fig.1b: Lopes & Rizzato**



**Fig.2: Lopes & Rizzato**

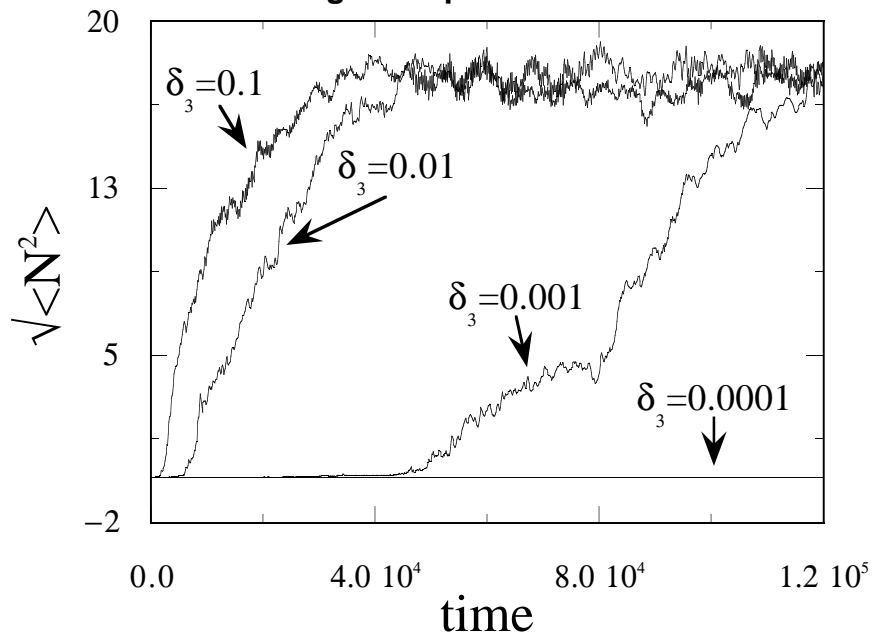


**Fig.3a: Lopes & Rizzato**

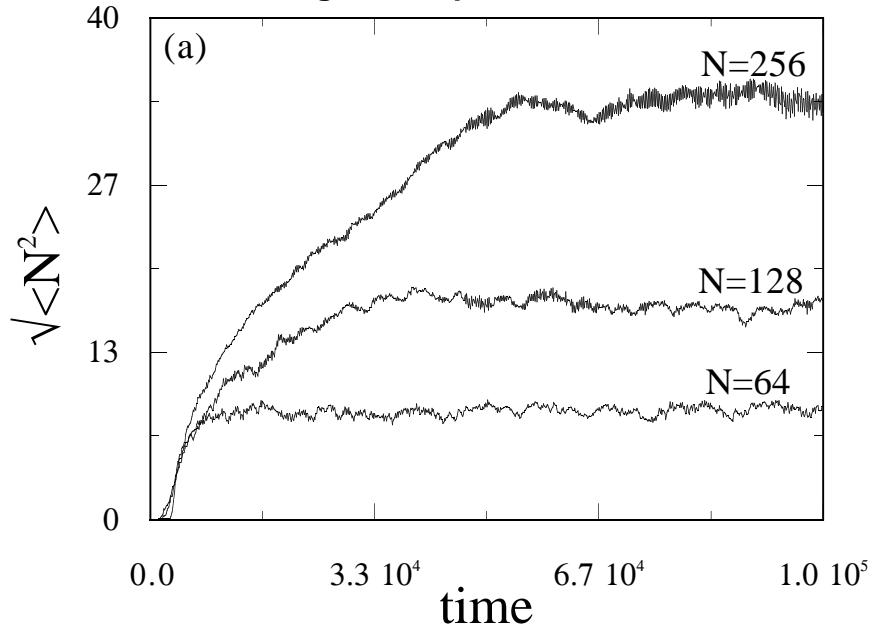


**Fig.3b: Lopes & Rizzato**

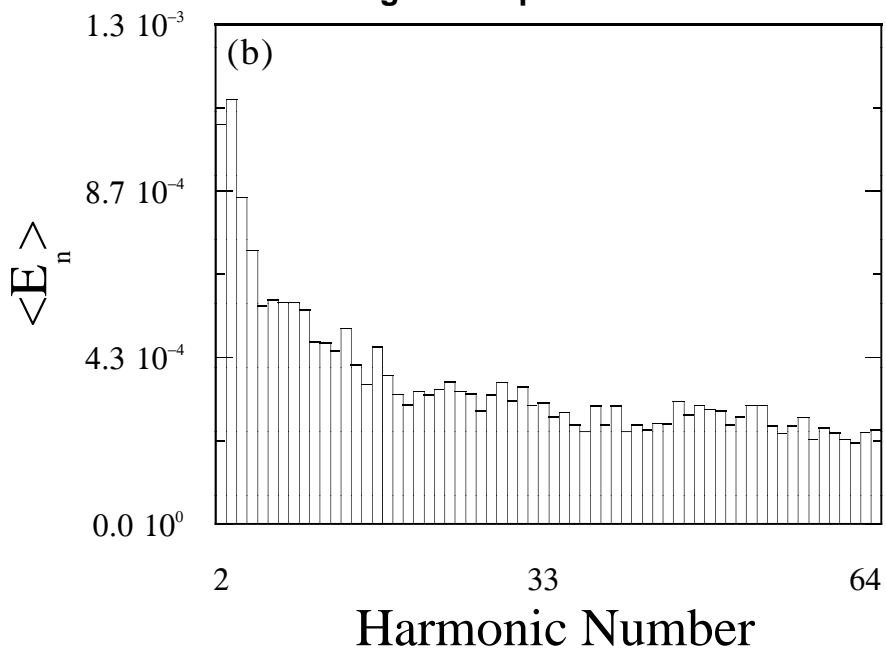


Fig.4:Lopes & Rizzato

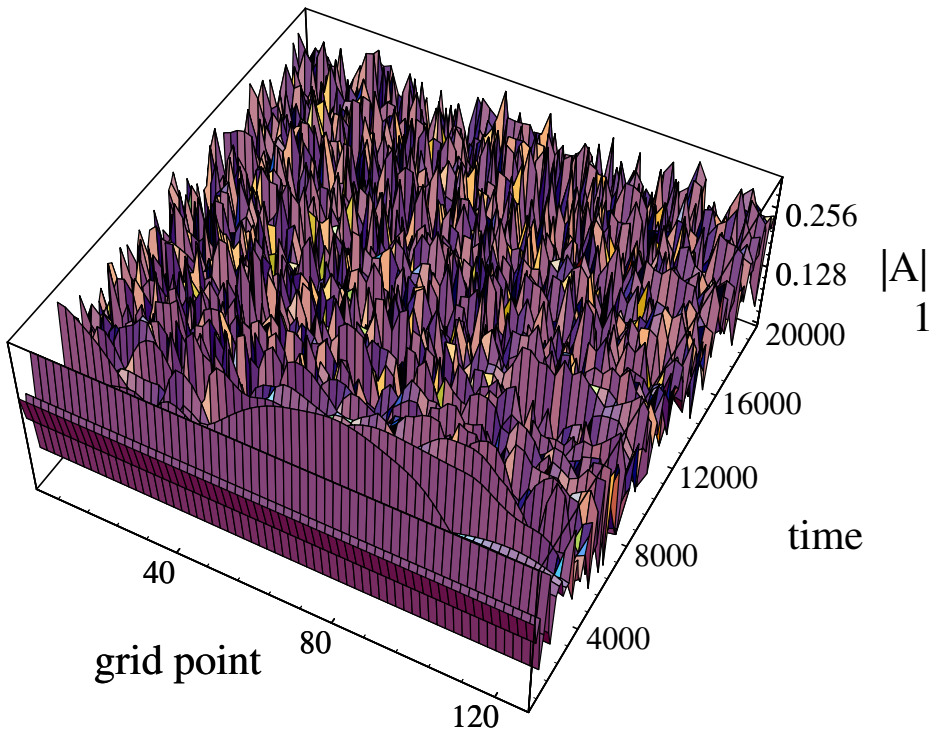


Fig.5: Lopes & Rizzato

